JOURNAL OF MATERIALS SCIENCE 19 (1984) 861–870

Analysis of the effect of embedded fibre length on fibre debonding and pull-out from an elastic matrix

Part 1 *Review of theories*

R. J. GRAY
Department of Civil Engineering, The University of British Columbia, Vancouver, British Columbia, Canada

The nature and properties of the resistance to fibre–matrix interfacial debonding in composites composed of ductile fibres in a brittle or elastic matrix can be determined using the single-fibre pull-out test. The results of such tests on cementitious matrix specimens indicate a non-linear relationship between the debonding and/or pull-out load and the embedded length of the fibre. Several of the theories developed to explain the debonding process and enable estimation of the parameters representing the debonding resistance through an analysis of pull-out test results are reviewed in this first of a two-part paper. The application of these theories to experimental data for steel fibre–cementitious matrix pull-out specimens is examined in the second part.

Nomenclature

b_i	effective thickness of the fibre–matrix interface
d_f	diameter of the fibre
l_c	embedded fibre length at which fibre fracture rather than pull-out occurs
l_d	debonded fibre length
l_e	embedded length of the fibre in a pull-out specimen
$l_{e,min}$	a minimum embedded fibre length which equals $(1/\alpha_2)\cosh^{-1}(\tau_{ib,max}/\tau_{ib,f})^{1/2}$
l_k	minimum embedded fibre length required to support the debonding stress in the fibre
l_p	maximum embedded fibre length at which complete debonding occurs instantaneously
$q_{ib,max}$	elastic shear flow resistance to fibre–matrix interfacial debonding
$q_{ib,f}$	frictional shear flow resistance to slipping at the fibre–matrix interface after the elastic bond has broken
r_f	radius of the fibre
r_m	effective radius of the matrix block in a pull-out test specimen
A_f	cross-sectional area of the fibre
A_m	cross-sectional area of the matrix block in a pull-out test specimen
C_1	a constant representing the normal compressive stress at the fibre–matrix interface
C_2	a constant representing the coefficient of friction between the fibre and the matrix at the interface
D	length of the "debonding plateau" (see Fig. 5a)
E_m	modulus of elasticity of the matrix
E_f	modulus of elasticity of the fibre
G_i	shear modulus of the fibre–matrix interface
G_m	shear modulus of the matrix
P_f	load applied to the fibre in a pull-out test
$P_{f,max}$	maximum load applied to the fibre in a pull-out test
$P_{f,ult}$	applied load at which fibre fracture occurs

0022–2461/84 $03.00 + .12

$P_{f,edb}$ load required to break the adhesional or elastic fibre–matrix interfacial bond in a pull-out test specimen

$P'_{f,edb}$ maximum value of $P_{f,edb}$ (see Fig. 7)

$P_{f,d}$ instantaneous decrease in applied fibre load when debonding is complete

$P_{f,r}$ residual fibre load required to overcome initial frictional resistance to fibre pull-out

$P_{f,\infty}$ applied fibre load required to debond an infinitely long fibre with no frictional resistance to slipping at the fibre–matrix interface

α an elastic constant
$\alpha_1 = (2G_i/b_i r_f E_f)^{1/2}$
$\alpha_2 = [(2\pi G_m/\ln(r_m r_f))(1/A_f E_f - 1/A_m E_m)]^{1/2}$
$\alpha_3 = [4\pi G_m/\ln(r_m/r_f) r_f E_f]^{1/2}$
$\alpha_4 = [G_m(A_f E_f + A_m E_m/A_f E_f A_m E_m)]^{1/2}$

γ_i surface energy of the fibre–matrix interface

δ_f fibre extension or displacement in a pull-out test

Δ slope of the linear portion of the $P_{f,max}$ against $\alpha_2 l_e$ curve and is equal to $\tau_{ib,f}\pi d_f/\alpha_2$

λ fibre–matrix misfit

μ coefficient of friction between the fibre and matrix at the interface

ν_f Poisson's ratio of the fibre

ν_m Poisson's ratio of the matrix

$\sigma_{f,max}$ stress in the fibre at which interfacial debonding occurs in a pull-out test specimen, i.e. debonding stress

$\sigma'_{f,max}$ plateau debonding stress (see Fig. 5b)

$\sigma_{f,po}$ stress in the fibre when fibre pull-out begins, i.e. immediately following the completion of interfacial debonding

$\sigma_{f,ult}$ ultimate tensile strength of the fibre

$\sigma_{i,n}$ normal compressive stress exerted by the matrix on the fibre across the interface

$\tau_{i,av}$ average shear stress at the fibre–matrix interface

$\tau_{i,max}$ maximum shear stress at the fibre–matrix interface

$\tau_{ib,av}$ average shear strength of the fibre–matrix interfacial bond

$\tau_{ib,max}$ maximum or adhesional shear strength of the fibre–matrix interfacial bond

$\tau_{ib,f}$ frictional resistance to slipping at the fibre–matrix interface after the elastic bond has broken

1. Introduction

Fundamental information on the nature and strength of the interfacial bond between the fibre and the matrix in a fibre-reinforced composite material can be obtained using the single-fibre, concentric pull-out test specimen and configuration shown schematically in Fig. 1. As noted previously by the present author [1], stress distributions in this specimen are the same as those within and on the surface of a fibre normal to and bridging a matrix crack in a composite which fails by matrix tensile fracture followed by fibre–matrix debonding* and fibre pull-out, i.e. the common failure mode for discontinuous fibre composites with a brittle or elastic matrix.

Resistance to the debonding and pull-out processes is principally a function of the fibre–matrix interfacial bond shear strength and the interfacial bond area, i.e. embedded fibre length times fibre diameter. Theoretical analyses of this resistance were initially developed for ductile or plastically deforming matrices and a uniform interfacial shear stress along the length of the embedded fibre was assumed. In this case, catastrophic failure of the interfacial bond occurs when its shear strength is reached and the debonding load, i.e. the peak load observed in the pull-out test, is directly proportional to the embedded fibre length. Experimental results for composites containing such matrices show agreement with this assumption [2–4].

However, theoretical analysis of the stress conditions in a pull-out test specimen with a brittle or elastic matrix show that the distribution of shear stress along the interface is not uniform, and that the relationship between the debonding and/or pull-out load and the embedded length of fibre in the specimen is more complex than indicated above. Furthermore, experimental results for steel fibre–cementitious matrix specimens in particular show that the variation of the peak pull-out load with embedded fibre length is nonlinear [5–8], and consequently it cannot be assumed that the true value of the interfacial bond shear strength can be obtained simply from this load and the nominal area of interfacial contact.

Several of the theories developed to describe and explain the variation of the debonding and/or pull-out load with embedded fibre length, and/or to relate the true value of the interfacial bond shear strength to the average value calculated from

*Debonding is herein defined as relative displacement or slip between the fibre and the matrix at the interface separating the two.

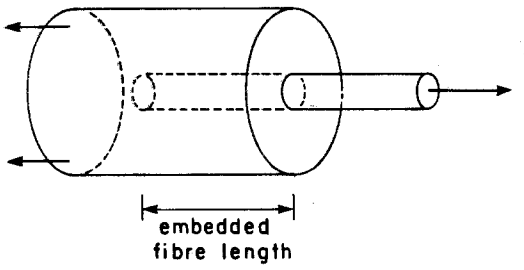

Figure 1 The single-fibre concentric pull-out test.

pull-out test results, for brittle or elastic matrices are examined in this paper. The applicability of these theories to pull-out test results for steel fibre–cementitious matrix specimens will be examined in a subsequent paper.

2. Theoretical analyses of pull-out test results†

A relationship between fibre–matrix interfacial shear stress and embedded fibre length in a pull-out test specimen has been developed by Greszczuk [9] using the assumptions of the shear lag theory, i.e. assuming that the extensional stresses in the matrix are negligible relative to those in the fibre and that the shear stresses in the fibre are small compared to those in the matrix. An element of the fibre in a model pull-out specimen and the corresponding boundary conditions are considered, see Fig. 2a, and it is shown that the maximum shear stress along the interface, $\tau_{i,max}$, occurs at the point where the fibre enters the matrix, i.e. at $x = 0$. This maximum shear stress is given by

$$\tau_{i,max} = \tau_{i,av}\alpha_1 l_e \coth \alpha_1 l_e \quad (1)$$

where $\tau_{i,av}$ is the average shear stress along the interface. As l_e approaches zero, the function $\alpha_1 l_e \coth \alpha_1 l_e$ approaches unity and hence the value of $\tau_{i,max}$ approaches that of $\tau_{i,av}$.

Greszczuk assumes that complete fibre–matrix debonding takes place when the maximum interfacial shear stress, $\tau_{i,max}$, is equal to the maximum interfacial bond shear strength, $\tau_{ib,max}$. For a given fibre embedment length, the average interfacial shear stress, $\tau_{i,av}$, at failure is then equal to the average interfacial bond shear strength, $\tau_{ib,av}$. This can be calculated from the pull-out test results using

$$\tau_{ib,av} = \frac{P_{f,max}}{\pi d_f l_e} \quad (2)$$

which assumes that the effect of bond, if any, between the fibre end and the matrix is negligible. Therefore, Equation 1 can be rewritten in the form

$$\tau_{ib,max} = \tau_{ib,av}\alpha_1 l_e \coth \alpha_1 l_e \quad (3)$$

and by analogy to the above, as l_e approaches zero, the value of $\tau_{ib,max}$ approaches that of $\tau_{ib,av}$.

For a given fibre and matrix, α_1 is assumed to be a constant and hence the ratio of $\tau_{ib,max}$ to $\tau_{ib,av}$ is a function of l_e only. An estimated value of $\tau_{ib,max}$ can therefore be obtained by: (1) testing pull-out specimens with various fibre embedment lengths, (2) calculating $\tau_{ib,av}$ values from the test results using Equation 2, (3) plotting these values as a function of l_e, and (4) extrapolating the resulting curve back to $l_e = 0$ as shown in Fig. 2b.

Rearrangement of Equation 3 to

$$\tau_{ib,av} = \frac{\tau_{ib,max}}{\alpha_1 l_e \coth \alpha_1 l_e}$$

shows that $\tau_{ib,av}$ is a function of l_e which decreases as l_e increases, as shown in Fig. 2b. It follows that the ratio $P_{f,max}/l_e$ decreases as l_e increases, and, as l_e becomes large, the slope of the curve relating $P_{f,max}$ to l_e becomes small. That is, the curve relating $P_{f,max}$ to l_e approaches some limiting value as l_e becomes large, as shown in Fig. 2c. The method employed to analyse pull-out test results for ductile or plastically deforming matrices assumes that $\tau_{ib,av}$ is constant, i.e. not a function of l_e, and hence there is a straight line relationship between $P_{f,max}$ and l_e as also shown in Fig. 2c.

As Lawrence [10] has pointed out, Greszczuk assumes that all of the fibre load is transferred to the surrounding matrix by adhesional or elastic "shear" forces at the interface and that immediate, catastrophic fibre–matrix debonding occurs when these shear forces are overcome. Lawrence, however, assumes that partial fibre–matrix debonding may occur, and takes the contribution to the load transfer process of frictional resistance forces acting over the debonded portion of the interface into account in his analysis. Using a model with the same geometry as that considered by Greszczuk, (Fig. 2a), it is shown that when the applied load is such that $\tau_{i,max} > \tau_{ib,max}$, the fibre starts to debond at the point where it enters the matrix. Whether debonding continues at this load or an increase in load is necessary depends on the

†It is generally assumed that the fibre is round and straight, i.e. undeformed, and is much more ductile than the matrix.

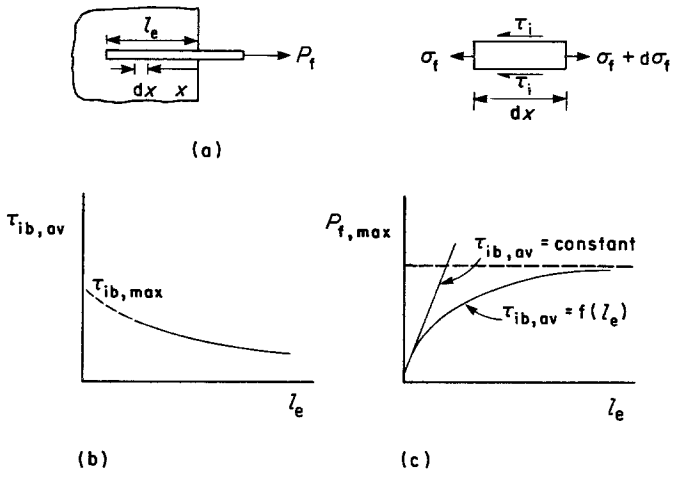

Figure 2 Fibre element in a pull-out test model and experimental results (after Greszczuk [9]). (a) Fibre element in pull-out model, (b) variation in average interfacial bond shear strength with embedded fibre length, and (c) variation in maximum pull-out load with embedded fibre length.

embedded length of the fibre, l_e, the ratio of the shear strength of the elastic interfacial bond, $\tau_{ib,max}$, to the frictional resistance to slipping after this bond has broken, $\tau_{ib,f}$, and a "minimum" embedded fibre length, $l_{e,min}$, which is also a function of the ratio $\tau_{ib,max}/\tau_{ib,f}$. For example, if $\tau_{ib,max}/\tau_{i,f} > 1$ and $l_e > l_{e,min}$, the debonding process is not catastrophic and a further increase in applied load is necessary to continue it. If however, $\tau_{ib,max}/\tau_{ib,f} > 1$ but $l_e < l_{e,min}$, debonding occurs catastrophically as soon as the applied load is such that $\tau_{i,max} > \tau_{ib,max}$. The maximum fibre load required to achieve complete debonding and initiate pull-out for these two cases is given by

$$P_{f,max} = \frac{\tau_{ib,max}\pi d_f}{\alpha_2}\tanh\alpha_2 l_e \qquad (4)$$

for ($l_e \leqslant l_{e,min}$), and

$$P_{f,max} = \frac{\tau_{ib,max}\pi d_f}{\alpha_2}\tanh\alpha_2 l_{e,min} + \tau_{ib,f}\pi d_f(l_e - l_{e,min}) \qquad (5)$$

where ($l_e > l_{e,min}$).

Once debonding has been completed, the resistance to fibre pull-out drops to a value of $\tau_{ib,f}\pi d_f l_e$, and subsequently decreases as the fibre is pulled out of the matrix.

To determine the maximum interfacial bond shear strength, $\tau_{ib,max}$, experimentally, the maximum pull-out load, $P_{f,max}$, for fibres of various embedded lengths, l_e, is measured and plotted against the function $\alpha_2 l_e$. The shape of the curve obtained is dependent upon the ratio $\tau_{ib,max}/\tau_{ib,f}$ as shown in Fig. 3. The form of the load against fibre displacement curve obtained in the pull-out test is also dependent on this ratio and schematic load–displacement curves for various ratios are shown in Fig. 4.

If the $P_{f,max}$ against $\alpha_2 l_e$ curve is a straight line, $\tau_{ib,max}/\tau_{ib,f} = 1$ and the interfacial resistance to debonding is purely frictional in nature. The shear stress along the interface can therefore be treated as a constant [11] and the "effective" shear strength of the bond can be calculated using Equation 2. Debonding is not catastrophic in this case, but, as shown in Fig. 4a, the pull-out load decreases linearly from the maximum applied load as the fibre is extracted from the matrix*.

For $1 < \tau_{ib,max}/\tau_{ib,f} < \infty$, the pull-out load against fibre displacement curve is shown in Fig. 4b. In this case, a point of discontinuity occurs on the $P_{f,max}$ against $\alpha_2 l_e$ curve (Fig. 3) at l_e equal to $l_{e,min}$ where the slope of the curve becomes con-

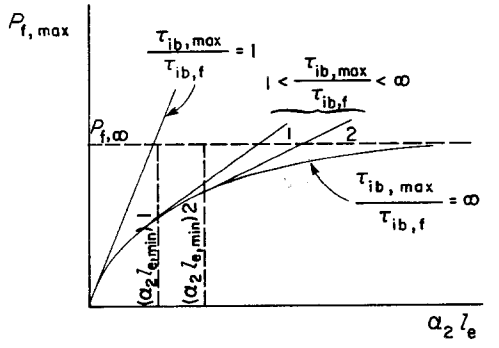

Figure 3 Variation of maximum pull-out load with embedded fibre length factor for various friction conditions (after Lawrence [10]).

*It is assumed that the coefficients of static and dynamic friction at the fibre–matrix interface are equal in value.

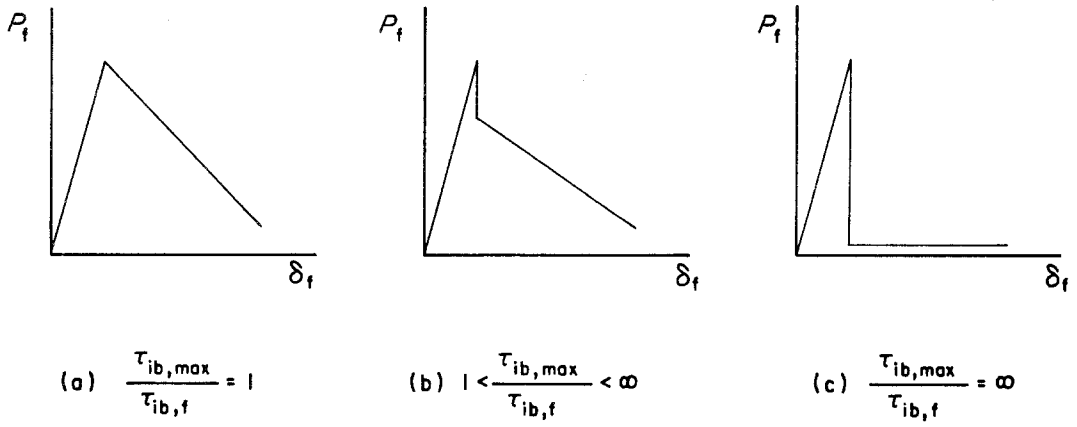

Figure 4 Variation of pull-out load with fibre displacement for various interfacial friction conditions.

stant. The slope, Δ, is related to the frictional resistance to fibre pull-out after complete debonding has occurred, and, according to Lawrence, can be set equal to $\tau_{ib,f}\pi d_f/\alpha_2$. Therefore

$$\tau_{ib,f} = \frac{\alpha_2\Delta}{\pi d_f} \quad (6)$$

and, from the definition if $l_{e,min}$, the maximum interfacial bond shear strength may be determined using

$$\tau_{ib,max} = \frac{\alpha_2\Delta}{\pi d_f}\cosh^2\alpha_2 l_{e,min} \quad (7)$$

where Δ and $l_{e,min}$ are obtained from the experimental curve of $P_{f,max}$ against $\alpha_2 l_e$.

If the curve relating the maximum pull-out load and the embedded fibre length has no obvious discontinuity and becomes approximately linear at long embedment lengths, then the frictional shear resistance is very small, Fig. 4c. Therefore $\tau_{ib,max}/\tau_{ib,f} \to \infty$ and all embedded fibre lengths are less than $l_{e,min}$. The maximum shear strength of the interfacial bond may be determined from the asymptote, $P_{f,\infty}$, of the experimental $P_{f,max}$ against $\alpha_2 l_e$ curve, since $\tanh\alpha_2 l_e \to 1$ as $l_e \to \infty$, and hence Equation 4 can be re-arranged to give

$$\tau_{ib,max} = \frac{P_{f,\infty}\alpha_2}{\pi d_f}. \quad (8)$$

Note that in Equation 4, as $l_e \to 0$, $\tanh\alpha_2 l_e \to \alpha_2 l_e$, and therefore $\tau_{ib,max} \to P_{f,max}/\pi d_f l_e$, which is equal to $\tau_{ib,av}$ according to Equation 2. This agrees with the proposition by Greszczuk [9], previously described, that $\tau_{ib,max}$ can be determined by extrapolating the experimental curve relating $\tau_{ib,av}$ and l_e back to $l_e = 0$.

Takaku and Arridge [12], like Greszczuk, do not take the contribution of frictional resistance forces acting over a debonded portion of the fibre–matrix interface into account in their derivation of the relationship between the maximum load required to cause debonding and the embedded fibre length. They also assume that the debonding process is catastrophic as soon as $\tau_{i,max} > \tau_{ib,max}$ at the point where the fibre enters the matrix, and they conclude that the relationship between $\tau_{ib,max}$ and l_e is the same as that developed by Greszczuk, that is

$$\tau_{ib,max} = \tau_{ib,av}\alpha_3 l_e \coth\alpha_3 l_e \quad (9)$$

with the exception that the elastic parameter, α_3, is defined differently.

By re-arranging Equation 9 and expressing $\tau_{ib,av}$ in terms of the maximum stress in the fibre when debonding occurs, $\sigma_{f,max}$, it is shown that:

$$\frac{\sigma_{f,max}}{2\tau_{ib,max}/r_f\alpha_3} = \tanh\alpha_3 l_e. \quad (10)$$

It is then assumed that $\tau_{ib,max}$ and α_3 are "adjustable" parameters which can be evaluated from the experimental results as follows. The relationship between $\tanh l_e$ and l_e, which is said to be a "normalized" curve representing Equation 10, and the experimental relationship between $\sigma_{f,max}$ and l_e are plotted on natural logarithmic paper. The "shift distances" required to superpose the experimental results on the normalized curve by moving them parallel to the vertical and horizontal axes are determined and set equal to $(2\tau_{ib,max}/r_f\alpha_3)^{-1}$ and α_3 respectively. The value of $\tau_{ib,max}$ can then be calculated from these results.

However, Takaku and Arridge have considered the resistance offered by frictional forces at the interface to fibre pull-out after complete debond-

ing has occurred, and have derived the following relationship between the initial pull-out stress in the fibre, $\sigma_{f,po}$, and l_e:

$$\sigma_{f,po} = C_1[1 - \exp(-C_2 l_e)] \quad (11)$$

where C_1, a function of the normal compressive stress exerted by the matrix on the fibre across the interface, $\sigma_{i,n}$, and the elastic properties of the fibre and matrix, is defined as

$$C_1 = \frac{\sigma_{i,n} E_f (1 + \nu_m)}{E_m \nu_f} \quad (12)$$

and C_2, a function of the coefficient of friction between the fibre and matrix at the interface, μ, and their elastic properties, is defined as

$$C_2 = \frac{2E_m \nu_f \mu}{E_f r_f (1 + \nu_m)}. \quad (13)$$

Values for C_1 and C_2 can be determined from the experimental relationship between $\sigma_{f,po}$ and l_e, and hence estimates of the values of $\sigma_{i,n}$ and μ can be obtained.

The transfer of stress between the fibre and the matrix due to frictional resistance to slipping at the interface subsequent to fibre–matrix debonding has been examined in some detail by Pinchin and Tabor [13, 14]. They propose that shrinkage of a cementitious matrix around an embedded fibre during curing results in a "misfit" between the fibre and the matrix and hence a compressive contact pressure normal to the interface. This contact pressure can be expressed in terms of the fibre–matrix misfit, λ, i.e. the difference between the radius of the fibre and the radius of the hole in the matrix in the absence of the fibre. The reduction in this compressive contact pressure as a result of lateral contraction of the fibre when subjected to a tensile pull-out load is also taken into account and the dependence of $\sigma_{f,po}$ on l_e is expressed in the same form as Equation 11 where

$$C_1 = \frac{\lambda E_f}{r_f \nu_f} \quad (14)$$

and

$$C_2 = \frac{2\nu_f \mu}{E_f r_f [(1 + \nu_m)/E_m + (1 + \nu_f)/E_f]}. \quad (15)$$

An estimate of the value of λ can be obtained from the experimental relationship between $\sigma_{f,po}$ and l_e.

Pull-out test results obtained by Pinchin and Tabor indicate, however, that shrinkage of the matrix also causes microcracks to form at the interface, and these result in a reduction in the frictional resistance to pull-out and non-linear or inelastic pull-out behaviour. Pull-out behaviour is further complicated by a "compaction" of the matrix adjacent to the fibre which effectively enlarges the fibre "hole" in the matrix and reduces the fibre–matrix misfit. This "compaction" is attributed to the pull-out process itself.

Pinchin and Tabor [13] also observed that shear failure occurred in the cementitious matrix adjacent to the fibre as well as at the fibre–matrix interface during the "debonding" and pull-out of fibres with "rough" surfaces. On this basis, they conclude that the adhesive shear strength of the fibre–matrix interfacial bond and the cohesive shear strength of the matrix are of a similar magnitude.

Bowling and Groves [15] have developed a model in which the debonding of a fibre of embedded length greater than a certain critical length occurs by the progression of a plastic yielded zone along the fibre at a constant debonding load. This load is a function of the stress required to produce sufficient radial contraction of the fibre to give its "rough" surface clearance from the matrix. Debonding ceases when a minimum length of the fibre, i.e. the critical length, l_k, which will just support this debonding load, remains in contact with the matrix. Pull-out of the fibre then occurs as this "plug" of unyielded material is withdrawn from the matrix.

Following a theoretical treatment of debonding originally proposed by Outwater and Murphy [16], Bowling and Groves express the "debonding stress", i.e. the stress in the fibre at the debonding load, as a function of the fibre–matrix interfacial surface energy, γ_i, and the resistance to shearing at the interface after debonding has occurred, taken here as $\tau_{ib,f}$, as follows:

$$\sigma_{f,max} = \left(\frac{4E_f \gamma_i}{r_f}\right)^{1/2} + \frac{2\tau_{ib,f} l_d}{r_f} \quad (16)$$

for $l_e > l_k$, where l_d is the debonded length of the fibre. At some value of l_d, l'_d, the debonding stress exceeds the yield stress of the fibre and the relatively large plastic radial contraction then reduces the interfacial frictional resistance over the length $(l_d - l'_d)$ to zero. Debonding continues at a constant load, resulting in a "debonding plateau" in the load–displacement curve as shown in Fig. 5a, the magnitude of which is determined by the plastic strain in the fibre needed to remove the

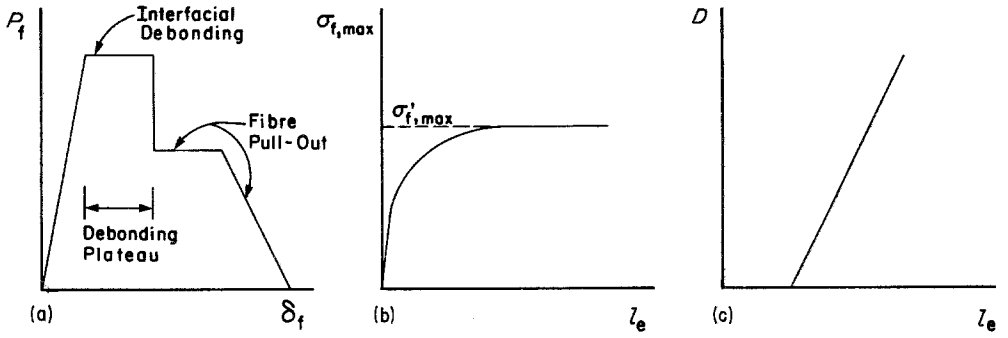

Figure 5 Experimental debonding and pull-out test results for a plastically deforming fibre (after Bowling and Groves [15]). (a) Fibre load–displacement curve, (b) variation of debonding stress with embedded fibre length, and (c) variation of debonding plateau length with embedded fibre length.

interfacial frictional resistance. The extent of this debonding plateau is related to the difference between l_e and l_k. Theoretical relations between (a) debonding stress, $\sigma_{f,max}$, and embedded fibre length, l_e, and (b) debonding plateau length, D, and embedded fibre length l_e, are shown in Figs. 5b and c respectively. Note that for fibres with $l_e < l_k$, these authors simply assume that "elastic" debonding occurs with the debonding stress increasing less-than-linearly with embedded fibre length.

The only measure of interfacial bond shear strength that can be obtained from an analysis of experimental pull-out test results on the basis of the model proposed by Bowling and Groves is an average value over the length l_k at the instant of final fibre debonding. This can be calculated from the plateau debonding stress, $\sigma'_{f,max}$, and the critical fibre pull-out length, l_k, as follows:

$$\tau_{ib,av} = \frac{2\sigma'_{f,max} r_f}{l_k}. \quad (17)$$

Values for $\sigma'_{f,max}$ and l_k can be estimated from pull-out test results presented as shown in Figs. 5b and c.

A graphical interpretation and analysis of pull-out test results for ductile fibres in a brittle matrix is proposed by Bartos [17]. Shear "flow", i.e. shear force per unit length, along the fibre–matrix interface is used rather than shear stress in order to avoid consideration of the reinforcing "fibre" perimeter, which is often difficult to determine, e.g. in the case of bundles of glass fibres. Non-uniform elastic and constant frictional shear flows are assumed to act along bonded and unbonded portions of the interface respectively. Debonding occurs when the maximum elastic shear flow equals the shear resistance per unit length of the bond – apparently any suitable theoretical model of the debonding process which is consistent with the fibre and matrix properties and the pull-out test configuration can be used to "express" the required debonding force, $P_{f,max}$.

The pull-out force–embedded fibre length diagram for a particular fibre–matrix combination is dependent upon the strength of the fibre and the characteristics of the interfacial bond. Typical $P_{f,max}$–l_e diagrams for a strong fibre and different interfacial bond conditions are shown in Fig. 6; in these diagrams, the tensile force required to break the fibre, $P_{f,ult}$, is represented by the straight line DF, and the force on the fibre required to break the elastic component of the interfacial bond, $P_{f,edb} = f(l_e)$, is represented by the curve OB. According to Bartos [17, 18], three different interfacial bond conditions can be identified as follows:

1. Elastic shear resistance to debonding only, with no assistant frictional resistance to slipping, i.e. $\tau_{ib,max} \neq 0$ with $\tau_{ib,f} = 0$, Fig. 6a. Fibres with embedment lengths $l_e < l_c$ debond instantly and pull out when the applied load reaches $P_{f,edb}$, but fibres with $l_e > l_c$ fail in tension without any previous debonding. An increase in the strength of the fibre, indicated by the straight line D'F', causes a rapid increase in l_e until all fibres debond and pull out regardless of their length.

2. No "elastic" bond at the interface, the load transfer being provided only by a uniform frictional resistance to slipping, i.e. $\tau_{ib,max} = 0$ but $\tau_{ib,f} \neq 0$, Fig. 6b. The greater the frictional resistance, the steeper the slope of the line OE and the shorter l_c.

3. A combination of "elastic" bonding and frictional resistance at the interface, i.e. $\tau_{ib,max} \neq 0$ and $\tau_{ib,f} \neq 0$, Fig. 6c. Depending upon the relative magnitudes of $P_{f,ult}$, $\tau_{ib,max}$, and $\tau_{ib,f}$, and upon

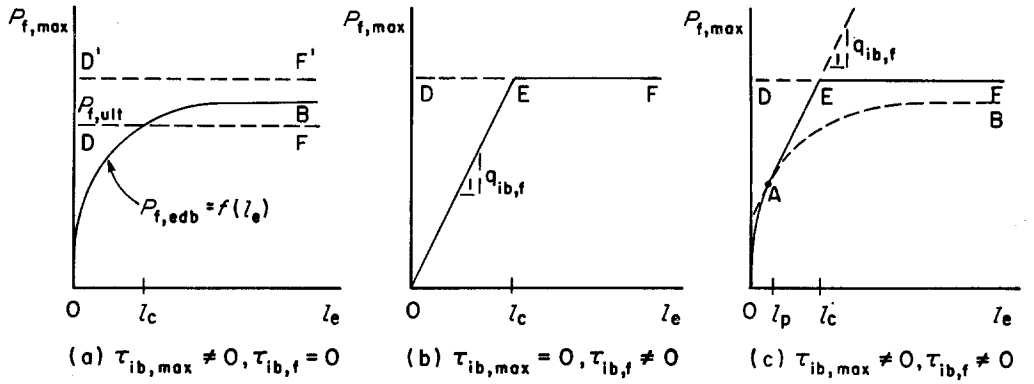

Figure 6 Variation of maximum pull-out load with embedded fibre length for various interfacial bond conditions (after Bartos [18]).

l_e, many modes of failure are possible; the following three are represented in Fig. 6c:

(a) $l_e < l_p$ – fibre–matrix debonding is complete and instantaneous and fibre pull-out occurs immediately.

(b) $l_p < l_e < l_c$ – gradual fibre–matrix debonding followed by instantaneous debonding and fibre pull-out.

(c) $l_c < l_e$ – gradual fibre–matrix debonding followed by tensile fracture of the fibre.

A relationship between pull-out load and embedded fibre length, apparently developed on the basis of a shear lag theory, is given by Barton [17] as

$$P_{f,max} = \frac{q_{ib,max}}{\alpha_4} \tanh \alpha_4 (l_e - l_d) + q_{ib,f} l_d \quad (18)$$

where $q_{ib,max}$ and $q_{ib,f}$ can be taken as equal to $\tau_{ib,max} \pi d_f$ and $\tau_{ib,f} \pi d_f$ respectively, and l_d is the length of the fibre which debonds before either complete fibre–matrix debonding and fibre pull-out or fibre failure occurs. If $l_e < l_p$, where l_p is the maximum embedded fibre length at which complete debonding occurs instantaneously, $l_d = 0$ and

$$P_{f,max} = \frac{q_{ib,max}}{\alpha_4} \tanh \alpha_4 l_e. \quad (19)$$

According to Bartos, sufficient information can be obtained from a single test in which a pull-out mode of failure is observed to determine l_c and l_p, and hence to obtain estimates of the values of $q_{ib,max}$ and $q_{ib,f}$, or $\tau_{ib,max}$ and $\tau_{ib,f}$ respectively. The values of $P_{f,max}$, $P_{f,d}$, i.e. the instantaneous drop in the applied load when debonding is complete, and $P_{f,r}$, i.e. the residual force required to overcome the initial frictional resistance to pull-out, can be obtained from the pull-out load–fibre displacement curve as shown in Fig. 7a. A point representing this test result (P) can then be plotted on a $P_{f,max}$ against l_e diagram, Fig. 7b. The slope

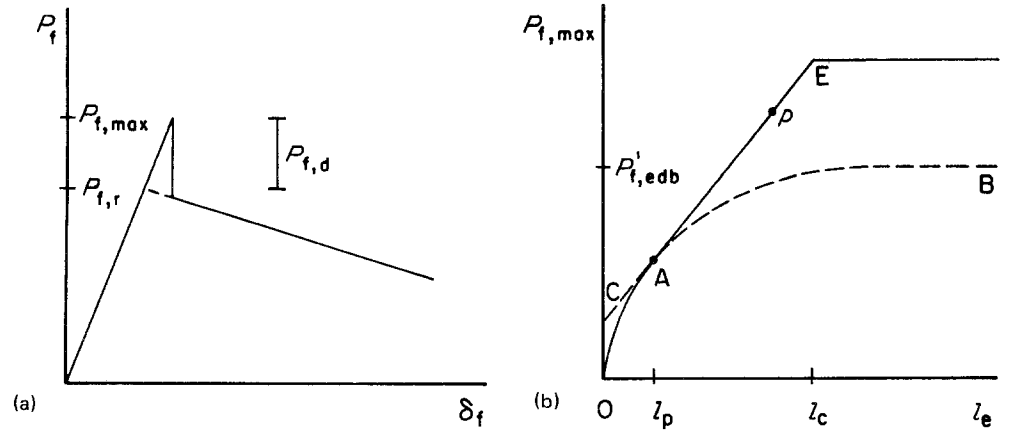

Figure 7 Experimental pull-out test result and analysis (after Bartos [17]). (a) Pull-out load–fibre displacement curve, and (b) maximum pull-out load-embedded fibre length diagram.

of the line CAE passing through P is

$$q_{ib,f} = \frac{P_{f,r}}{l_e}. \quad (20)$$

The curved line, OAB, representing

$$P_{f,edb} = \frac{q_{ib,max}}{\alpha_4} \tanh \alpha_4 l_e \quad (21)$$

is tangent to line CAE at A, and can be determined using either a graphical or numerical curve-fitting technique. Note that OAB is assumed to reach some constant load value, identified here as $P'_{f,edb}$, as l_e becomes large; hence $q_{ib,max}$ can be obtained by re-arranging Equation 19 and substituting for $P_{f,max}$ and $\tanh \alpha_4 l_e$, i.e.

$$q_{ib,max} = \alpha_4 P'_{f,edb}. \quad (22)$$

Laws [19] has extended Lawrence's analysis to show that the pull-out load–fibre displacement curve has the shape shown schematically in Fig. 8. The initial linear portion of this curve, to point A, represents the elastic extension of the fibre while the bond is still intact. Subsequent debonding is either catastrophic, the fibre pulling out without a further increase in load (solid line), or is progressive, an increase in load being required to overcome additional frictional resistance forces and achieve complete debonding (dashed line). In the latter case, after the maximum load is reached, point B, the load decreases until debonding is complete, point C. This debonding is accompanied by a decrease in fibre extension, which is not usually observed because pull-out tests are normally conducted under constant rate of extension conditions; instead, the load usually drops suddenly from its maximum value to a value corresponding to that extension on the post-debond part of the pull-out load–fibre displacement curve (see Fig. 4b).

Values for $\tau_{ib,max}$ and $\tau_{ib,f}$ can be obtained from the pull-out load–fibre displacement curve if points A and C can be identified since, according to Laws, at point A where debonding begins,

$$P_f = \frac{\tau_{ib,max} \pi d_f}{\alpha_2} \tanh \alpha_2 l_e \quad (23)$$

and at point C where debonding is complete,

$$P_f = \tau_{ib,f} \pi d_f l_e. \quad (24)$$

A value of $\tau_{ib,av}$ can be calculated from the maximum pull-out load, point B, using Equation 2, and this is noted as being less than $\tau_{ib,max}$ but greater

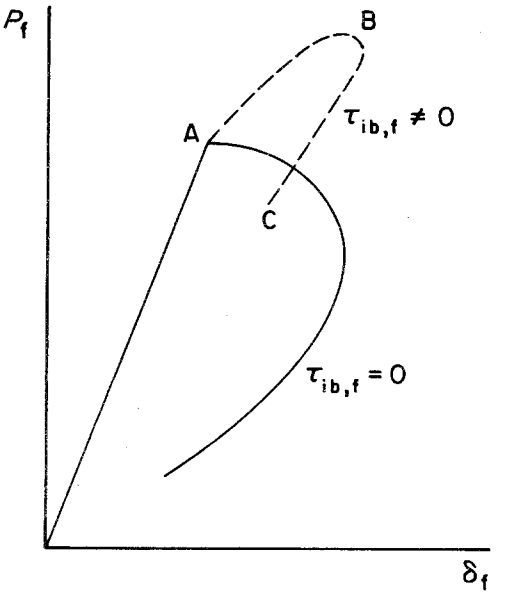

Figure 8 Theoretical pull-out load–fibre extension/displacement cuves (after Laws [19]).

than $\tau_{ib,f}$. However, $\tau_{ib,av} \rightarrow \tau_{ib,max}$ as $l_e \rightarrow 0$, although the difference can be large for even very short pull-out lengths, and $\tau_{ib,av} \rightarrow \tau_{ib,f}$ as $l_e \rightarrow \infty$. Laws regards the maximum interfacial bond shear strength, $\tau_{ib,max}$, as the sum of the strengths of a "chemical and cohesive bond" and a "frictional bond", i.e. the frictional resistance to slipping at the interface, $\tau_{ib,f}$, rather than as simply the strength of an adhesional bond between the fibre and the matrix. Hence a value for the "chemical or cohesive bond" can be obtained by taking the difference between $\tau_{ib,max}$ and $\tau_{ib,f}$.

Finally, Laws notes that although it is possible theoretically to calculate numerical values for the parameters representing resistance to debonding at the fibre–matrix interface from pull-out test results, these values apply to the conditions in the pull-out test, but not necessarily to those in a test of a specimen of the composite material consisting of the same fibre and matrix.

3. Conclusions

The evolvement of theoretical treatments of the resistance to the fibre–matrix debonding and fibre pull-out processes in ductile fibre–brittle matrix composite systems, and of the associated analyses of the effects of parameters such as embedded fibre length, has apparently proceeded in a rational manner. Most of the more recent treatments are essentially extensions and/or refinements of earlier ones. In particular, since the recognition by

Lawrence [10] that frictional resistance to slipping over a debonded portion of the interface can contribute significantly to the total resistance to debonding, the major effort has been directed at developing appropriate methods for treating experimental data, i.e. pull-out test results, to determine the nature and properties of the total debonding resistance of a particular fibre–matrix combination.

The principal characteristics of the majority of the theories with respect to their treatment of the nature of fibre–matrix debonding in general, and of the effect of the embedded length of the fibre on the debonding and pull-out processes in particular, can be summarized as follows:

1. There are two types of resistance to fibre–matrix interfacial debonding: adhesional or elastic bonding, and frictional resistance to slipping. The total resistance to debonding and the nature of the debonding process are determined by the particular combination of these two types that occurs in a pull-out test specimen.

2. The mixture of adhesional bonding and frictional resistance that occurs in a pull-out test specimen is very strongly dependent upon the embedded length of the fibre – the contribution of elastic/adhesional bonding to the total resistance to debonding decreases as embedded fibre length increases, whereas the contribution of the frictional resistance to slipping increases. The force and energy required to cause debonding can be maximized by optimizing the embedded fibre length.

3. The process of fibre–matrix debonding can be assessed and numerical estimates of the parameters representing debonding resistance, i.e. maximum interfacial bond shear strength ($\tau_{ib,max}$) and/or frictional resistance to slipping ($\tau_{ib,f}$), can be obtained by analysis of the relationship between pull-out load and fibre displacement and/or between maximum pull-out load and embedded fibre length determined from pull-out tests.

The major differences between the more complex of these theories are: (a) the definition of the elastic constant, α, involved in the expression of the relationship between fibre load and embedded length, and (b) the actual method of treating the experimental data to obtain numerical estimates of the debonding resistance parameters.

References

1. R. J. GRAY and C. D. JOHNSTON, in Proceedings of the RILEM Symposium on Testing and Test Methods of Fibre Cement Composites, The University of Sheffield, April 1978, edited by R. N. Swamy (The Construction Press, Lancaster, 1978) p. 317.
2. A. KELLY and W. R. TYSON, in "High Strength Materials", edited by V. F. Zackay (John Wiley and Sons, New York, 1965) p. 578.
3. L. J. BROUTMAN, in "Interfaces and Composites" ASTM STP 452 (American Society for Testing and Materials, Philadelphia, 1969) p. 27.
4. G. A. COOPER, *J. Mater. Sci.* **5** (1970) 645.
5. B. P. HUGHES and N. I. FATTUHI, *Mag. Concrete Res.* **27** (1975) 1749.
6. M. MAAGE, *Cem. Concrete Res.* **7** (1977) 703.
7. P. W. R. BEAUMONT and J. C. ALESZKA, *J. Mater. Sci.* **13** (1978) 161.
8. R. J. GRAY, PhD thesis, The University of Calgary (1982).
9. L. B. GRESZCZUK, in "Interfaces in Composites" ASTM STP 452 (American Society for Testing and Materials, Philadelphia, 1969) p. 42.
10. P. LAWRENCE, *J. Mater. Sci.* **7** (1972) 1.
11. V. LAWS, P. LAWRENCE and R. W. NURSE, *J. Phys. D: Appl. Phys.* **6** (1973) 523.
12. A. TAKAKU and R. G. C. ARRIDGE, *ibid* **6** (1973) 2038.
13. D. J. PINCHIN and D. TABOR, *Cem. Concrete Res.* **8** (1978) 139.
14. *Idem, J. Mater. Sci.* **13** (1978) 1261.
15. J. BOWLING and G. W. GROVES, *ibid.* **14** (1979) 431.
16. J. D. OUTWATER and M. C. MURPHY, in Proceedings of the 24th Annual Technical Conference of the Reinforced Plastics/Composites Division, The Society of the Plastics Industry, Inc., Washington, DC, 1969, p. 11-C.
17. P. BARTOS, *J. Mater. Sci.* **15** (1980) 3122.
18. *Idem, Int. J. Cem. Composites Lightweight Aggregates* **3** (1981) 145.
19. V. LAWS, *Composites* **13** (1982) 145.

Received 7 April
and accepted 1 July 1983